

Collisional oscillations of trapped boson-fermion mixtures approaching collapse

P. Capuzzi, A. Minguzzi, and M. P. Tosi

NEST-INFM and Classe di Scienze, Scuola Normale Superiore, Piazza dei Cavalieri 7, I-56126 Pisa, Italy

(Dated: February 8, 2020)

We study the collective modes of a confined gaseous cloud of bosons and fermions with mutual attractive interactions at zero temperature. The cloud consists of a Bose-Einstein condensate and a spin-polarized Fermi gas inside a spherical harmonic trap and the coupling between the two species is varied by increasing either the magnitude of the interspecies s -wave scattering length or the number of bosons. The mode frequencies are obtained in the collisional regime by solving the equations of generalized hydrodynamics and are compared with the spectra calculated in the collisionless regime within a random-phase approximation. We find that, as the mixture is driven towards the collapse instability, the frequencies of the modes of fermionic origin show a blue shift which can become very significant for large numbers of bosons. Instead the modes of bosonic origin show a softening, which becomes most pronounced in the very proximity of collapse. Explicit illustrations of these trends are given for the monopolar spectra, but similar trends are found for the dipolar and quadrupolar spectra except for the surface ($n = 0$) modes which are essentially unaffected by the interactions.

PACS numbers: 03.75.Kk, 03.75.Ss, 67.60.-g

I. INTRODUCTION

Boson-fermion mixtures have been produced with atomic gases in several experiments [1, 2, 3, 4, 5, 6] and the deep quantum-degeneracy regime has been reached for both the bosonic and the fermionic component [7, 8]. The aim of fermion cooling in these mixtures has been the realization of a superfluid state [9, 10]. Even though the mixtures are very dilute, the interactions between bosons and fermions play important roles and in particular the s -wave collisions between the two species are exploited in the evaporative cooling process to obtain rethermalization. Mean-field interactions affect the expansion rate of the cloud and its thermodynamic properties [5, 11].

For a ^{87}Rb - ^{40}K mixture the boson-fermion interactions are large and attractive [12], while in other systems they could be tuned to become attractive by exploiting Feshbach resonances [13, 14, 15]. Boson-fermion attractions enhance the overlap between the two species, favoring in principle a boson-mediated fermion pairing [16, 17], and ultimately lead to the collapse of the cloud as the boson-fermion coupling strength overcomes the Fermi pressure. Collapse has been observed experimentally in the ^{87}Rb - ^{40}K mixture as a sudden disappearance of the fermion cloud when the number of bosons, and hence the coupling between the two species, is increased [18]. The equilibrium properties and the phase diagram of a mixture with attractive interactions have been investigated by several authors [19, 20, 21, 22], finding good agreement between the experimental data and a mean-field theoretical description [23, 24].

The study of the collective modes of a boson-fermion mixture with repulsive interactions has proved to be a good indicator of the quantum transition to a spatially demixed state [25]. For the case of attractive interactions some analyses using semi-analytical methods [26, 27] have suggested that the lowest-lying monopolar mode should show a softening in the approach to collapse. A

similar frequency softening is found for a pure condensate with increasingly large boson attractions [28, 29]. In contrast, the numerical solution of the equations of motion for boson-fermion mixtures in the collisionless Random-Phase-Approximation (RPA) does not give indications of frequency softening for the choice of parameters adopted in the calculations [30]. Moreover, it is found that when the number of bosons is much larger than that of fermions some families of modes are strongly blue-shifted as a consequence of the increase of the particle densities in the cloud approaching collapse [31]. However, the RPA calculations could not be brought to the very proximity of collapse because of very severe numerical difficulties.

In this paper we study the collective modes of a trapped boson-fermion mixture with attractive interactions using the equations of generalized hydrodynamics. These allow us to span the entire range of boson-fermion interaction strength up to the collapse point. Although the hydrodynamic equations are strictly valid only in the collisional regime, their predictions also serve as a guideline to interpret the RPA spectra. By evaluating the frequencies of the first ten low-lying modes we find that some modes undergo a blue shift which can become quite large at large numbers of bosons, while some other modes display a softening which becomes pronounced in a very narrow window in the proximity to collapse.

II. EQUATIONS OF GENERALIZED HYDRODYNAMICS

We consider a model for a dilute mixture of two species of alkali atoms inside harmonic traps, one species being spin-polarized fermions of mass m_F and the other bosons of mass m_B . The boson-boson and boson-fermion interactions are described by contact potentials involving the coupling constants $g_{BB} = 4\pi\hbar^2 a_{BB}/m_B$ and $g_{BF} = 2\pi\hbar^2 a_{BF}/m_r$, where a_{BB} and a_{BF} are the corresponding

s -wave scattering lengths and $m_r = m_B m_F / (m_F + m_B)$. The fermion-fermion interactions are negligible, since the Pauli principle forbids collisions in the s -wave channel between fermions of the same spin. In the following we treat the case of boson-fermion attractions ($a_{BF} < 0$) and boson-boson repulsions ($a_{BB} > 0$).

The dynamics of the mixture in the collisional regime is described by the equations of generalized hydrodynamics as in Ref. [25]. These are (i) the equations for particle conservation,

$$\partial_t \rho_\sigma + \nabla \cdot \mathbf{j}_\sigma = 0, \quad (1)$$

relating the particle density $\rho_\sigma(\mathbf{r}, t)$ to the current density $\mathbf{j}_\sigma(\mathbf{r}, t)$ for each component ($\sigma = B, F$); and (ii) the quantum Navier-Stokes equations for momentum conservation, which are

$$m_\sigma \partial_t \mathbf{j}_\sigma = \rho_\sigma (\mathbf{F}_\sigma - \nabla V_\sigma - g_{BF} \nabla \rho_{\bar{\sigma}}) \quad (2)$$

to linear order in the velocity fields. Here $\bar{\sigma}$ denotes the component different from σ , $V_\sigma(\mathbf{r}) = m_\sigma \omega_\sigma^2 r^2 / 2$ are isotropic trapping potentials, and $\mathbf{F}_\sigma(\mathbf{r}, t)$ are self-consistent internal forces. We take for the latter the expressions

$$\mathbf{F}_B = -\nabla \left[g_{BB} \rho_B - \frac{\hbar^2}{2m_B} \frac{\nabla^2 \sqrt{\rho_B}}{\sqrt{\rho_B}} \right] \quad (3)$$

and

$$\mathbf{F}_F = -\nabla \left[A \rho_F^{2/3} - \frac{\hbar^2}{6m_F} \frac{\nabla^2 \sqrt{\rho_F}}{\sqrt{\rho_F}} \right], \quad (4)$$

with $A = \hbar^2 (6\pi^2)^{2/3} / 2m_F$. The equations of generalized hydrodynamics are thereby closed by means of a local-density approximation on the kinetic stress tensors, which also includes surface kinetic contributions through the last term on the rhs of Eqs. (3) and (4) [25]. These surface correction terms transcend the standard Thomas-Fermi approximation and for bosons the present approach is in fact equivalent to the full time-dependent Gross-Pitaevskii equation.

The equilibrium state of the mixture is given by the stationary solutions of Eq. (2). These also correspond to a minimum of the energy functional

$$\begin{aligned} E[\rho_B, \rho_F] = & \int d^3r \left(V_B \rho_B + \frac{g_{BB}}{2} \rho_B^2 + \xi_B \right) \\ & + \int d^3r \left(V_F \rho_F + \frac{3}{5} A \rho_F^{5/3} + \xi_F \right) \\ & + g_{BF} \int d^3r \rho_F \rho_B, \end{aligned} \quad (5)$$

where the surface kinetic-energy terms are $\xi_B = \hbar^2 |\nabla \sqrt{\rho_B}|^2 / 2m_B$ and $\xi_F = \hbar^2 |\nabla \sqrt{\rho_F}|^2 / 6m_F$.

At increasingly large boson-fermion attractions the densities of the two species increase in their overlap region and collapse occurs when these attractions overcome

the Fermi kinetic pressure and the boson-boson repulsions. Collapse is identified in the numerical search for the equilibrium state as the point where it is no longer possible to find a stable minimum for the energy functional in Eq. (5). We have verified that the location of collapse found in this way is well approximated by the estimate [19, 32]

$$|a_{BF}^c| = \left(\frac{a_{BB}}{\alpha k_F} \right)^{1/2}, \quad (6)$$

where $k_F = (6\pi^2 \rho_F(0))^{1/3}$ is the Fermi wave number estimated from the fermion density at the center of the trap and $\alpha = [3^{1/3} / (2\pi)^{2/3}] (m_F + m_B)^2 / (4m_F m_B)$.

In the following we characterize the approach of the mixture to the collapse instability by following the behavior of its low-lying collective oscillation frequencies. The normal modes of Eqs. (1) and (2) are found by expanding $\rho_\sigma(\mathbf{r}, t)$ around the equilibrium state $\rho_\sigma^0(r)$ as $\rho_\sigma(\mathbf{r}, t) = \rho_\sigma^0(r) + \delta\rho_\sigma(\mathbf{r}) e^{i\omega t}$, linearizing Eqs. (1) and (2), and Fourier transforming with respect to the time variable. This yields the coupled eigenvalue equations

$$m_\sigma \omega^2 \delta\rho_\sigma = \nabla \cdot (\rho_\sigma^0 \delta\mathbf{F}_\sigma) - g_{BF} \nabla \cdot (\rho_\sigma^0 \nabla \delta\rho_{\bar{\sigma}}), \quad (7)$$

where $\delta\mathbf{F}_\sigma$ are the forces obtained as $\delta\mathbf{F}_\sigma = \mathbf{F}_\sigma[\rho_\sigma^0 + \delta\rho_\sigma] - \mathbf{F}_\sigma[\rho_\sigma^0]$ to linear order in the density fluctuations (for their expressions see Ref. [25]). We also determine the solutions of the eigenvalue equations in the case where the dynamical coupling between the two components is neglected. Hereafter we shall call these solutions the uncoupled boson and fermion modes and calculate them by solving Eq. (7) for $\sigma = B$ and F with the second term in the rhs set to zero. This calculation will help us in attributing bosonic or fermionic character to the coupled modes of the mixture by comparison with the frequencies of the uncoupled modes. Even though the bosonic and fermionic oscillations that are obtained in this way are dynamically uncoupled, the effect of the mutual boson-fermion interaction is included in their calculation through the use of the density profiles of the mixture at equilibrium.

The numerical procedure that we have used can be summarized as follows: (i) we find the equilibrium density profiles by minimizing the energy functional (5) using the steepest-descent method; (ii) we project Eq. (7) into subspaces of different angular momentum l by factorizing the density fluctuations as $\delta\rho_\sigma(\mathbf{r}) = \delta\rho_\sigma^l(r) Y_{lm}(\hat{r})$ where $Y_{lm}(\hat{r})$ are the spherical harmonics; and (iii) we solve the coupled equations in a given l -subspace by means of standard linear-algebra routines [33].

III. COLLECTIVE MODES

We have solved Eq. (7) for two sets of experimentally relevant system parameters, corresponding to a ${}^7\text{Li}$ - ${}^6\text{Li}$ mixture [4] and to a ${}^{87}\text{Rb}$ - ${}^{40}\text{K}$ mixture [18]. In both cases we have set the frequency of the isotropic trap at

the geometric average of the frequencies in the experimental setup and have adopted the experimental value of the boson-boson scattering length. In our calculations we follow two different routes to reach collapse. We drive the ${}^7\text{Li}$ - ${}^6\text{Li}$ mixture to collapse by varying the value of a_{BF} from positive to strongly negative, as could be achieved by means of a Feshbach resonance. In the ${}^{87}\text{Rb}$ - ${}^{40}\text{K}$ mixture instead we keep a_{BF} fixed and increase the number N_B of bosons, as is done in the experiments of Modugno *et al.* [18].

A. The ${}^7\text{Li}$ - ${}^6\text{Li}$ mixture

Figure 1 shows the frequencies of the low-lying monopole ($l = 0$) modes in the ${}^7\text{Li}$ - ${}^6\text{Li}$ mixture as functions of a_{BF} , with the choice of parameters $\omega_F = \omega_B = 2\pi \times 1000 \text{ s}^{-1}$, $a_{BB} = 0.27 \text{ nm}$, and particle numbers $N_F = 10^4$ and $N_B = 10^6$. Pronounced blue shifts are observed at intermediate values of the boson-fermion scattering length both in a set of eigenfrequencies of Eq. (7) (circles) and in the frequencies of the uncoupled fermionic modes (dashed lines). This effect is a consequence of the increase of fermion density in the central part of the trap as the strength of the coupling is increased. For our choice of parameters the bosonic density profile is almost unaffected in this range of boson-fermion coupling and essentially acts as an effective attractive well for the fermions. The proximity of these modes to the uncoupled fermionic modes indicates that the effect of the dynamical coupling is negligible, thus confirming the interpretation in terms of static mean-field effects. At larger values of $|a_{BF}|$ the other eigenfrequencies of Eq. (7) (circles) show an increasing departure from the uncoupled bosonic modes (solid lines) and tend to rapidly soften as collapse is approached. We conclude that, in contrast to the blue-shift of the fermionic modes, the softening of “bosonic” modes is a truly dynamical signature of the impending collapse.

Similar trends of the mode frequencies are also found for the dipole ($l = 1$) and quadrupole ($l = 2$) oscillations, except that the lowest ($n = 0$) mode is in both cases essentially unaffected by the interactions. For the dipole mode this behavior is an exact consequence of the generalized Kohn theorem [34, 35], while for modes of higher l it is strictly valid only in the Thomas-Fermi limit. This can be explicitly verified from Eq. (7) by making the Ansatz $\delta\rho_\sigma(\mathbf{r}) \propto r^l Y_{lm}(\hat{r})$ for the density fluctuations and by exploiting the property $\nabla^2 \delta\rho_\sigma = 0$ for these modes.

B. The ${}^{87}\text{Rb}$ - ${}^{40}\text{K}$ mixture

We evaluate the collective modes of a ${}^{87}\text{Rb}$ - ${}^{40}\text{K}$ mixture with scattering lengths $a_{BB} = 5.5 \text{ nm}$ and $a_{BF} = -21.7 \text{ nm}$. Although both components are inside the same magnetic trap, their trapping frequencies differ

considerably as a consequence of the large difference in atomic masses. In the numerical calculations we take $\omega_B = 2\pi \times 90.9 \text{ s}^{-1}$ and $\omega_F = 2\pi \times 134 \text{ s}^{-1}$. Collapse is approached by varying N_B from 4×10^3 to approximately 8×10^4 , while keeping $N_F = 2 \times 10^4$ fixed.

In Fig. 2 we show the frequencies of the low-lying monopolar modes for this mixture. At increasing values of the boson number we find that the frequencies of the bosonic modes, identified as those that are closer to the uncoupled bosonic fluctuations, show a monotonic decrease which becomes very pronounced very close to collapse. On the other hand, the fermionic modes only show a modest blue shift. This is not as large as in our results for the ${}^7\text{Li}$ - ${}^6\text{Li}$ mixture, since the numbers of particles of the two species are here more similar.

IV. SPECTRAL FUNCTIONS

We have also calculated the whole spectral functions under the effect of the perturbing fields $\delta U_\sigma(\mathbf{r})e^{i\omega t}$, in order to make a comparison of the collisional spectra with those of the mixtures in the RPA collisionless regime. Peaks in the spectral functions indicate the location of collective modes, while their height measures the probability of a transition from the equilibrium state to an excited state with energy $\hbar\omega$.

In the collisional regime the spectral peaks are located in correspondence of the eigenfrequencies ω_i of Eq. (7), while the strength of a transition at a frequency ω is estimated from the corresponding density fluctuations $\delta\rho_\sigma^i(\mathbf{r})$ as

$$S_{\sigma\sigma'}^{\text{coll}}(\omega) = -\frac{1}{\pi} \text{Im} \sum_i \frac{\mathcal{Z}_{\sigma'}^i}{\omega_i^2 - \omega^2} \int d^3r \delta U_\sigma^*(\mathbf{r}) \delta\rho_{\sigma'}^i(\mathbf{r}) \quad (8)$$

(see Appendix). Here the sum is performed over the whole spectrum of Eq. (7) and \mathcal{Z}_σ^i is given by

$$\mathcal{Z}_F^i = \frac{2A}{3m_F} \int d^3r (\rho_F^0)^{-1/3} \delta\rho_F^i \nabla \cdot (\rho_F^0 \nabla \delta U_F) \quad (9)$$

and

$$\mathcal{Z}_B^i = \frac{g_{BB}}{m_B} \int d^3r \delta\rho_B^i \nabla \cdot (\rho_B^0 \nabla \delta U_B). \quad (10)$$

Since we are using in Eq. (8) the equilibrium profiles and the mode frequencies of the fully coupled dynamical equations, we expect it to yield the spectral functions quite accurately.

More generally, the spectral functions are related to the density-density responses $\chi_{\sigma\sigma'}(\mathbf{r}, \mathbf{r}', \omega)$ by the fluctuation-dissipation theorem,

$$S_{\sigma\sigma'}(\omega) = -\frac{1}{\pi} \text{Im} \int d^3r d^3r' \delta U_\sigma^*(\mathbf{r}) \chi_{\sigma\sigma'}(\mathbf{r}, \mathbf{r}', \omega) \delta U_{\sigma'}(\mathbf{r}'). \quad (11)$$

We evaluate the response functions in the collisionless regime within the RPA, following the approach described

in Refs. [31, 36]. For a monopolar drive ($\delta U_\sigma(\mathbf{r}) \propto r^2$) we calculate both the fermionic response $S_{FF}^{l=0}(\omega)$ and the bosonic response $S_{BB}^{l=0}(\omega)$, corresponding to excitations induced by applying the drive separately on the fermions or on the bosons.

In Figs. 3 and 4 we report the spectral functions of the ${}^7\text{Li}-{}^6\text{Li}$ mixture as obtained from the RPA formalism (top panels) and from Eq. (8) for the collisional regime (bottom panels) at various values of a_{BF} and with the same choice of parameters as in Fig. 1. In the absence of boson-fermion coupling a fermionic perturbing field excites the pure $n = 0$ mode of the fermions, which gives the only contribution to the FF spectra. In contrast, the BB spectra contain in the same limit several weak peaks at higher frequencies above the pure $n = 0$ mode of the bosons, owing to the boson-boson interactions. For $a_{BF} \neq 0$ the RPA spectra are very complex, from the lifting of degeneracy in the discrete-level structure which is due to the interactions with the bosons. The fermionic peaks can be recognized as broad fragmented contributions of largest height in the fermionic spectral functions, while the bosonic peaks are usually isolated and are most marked in the bosonic spectra [31].

Quite interestingly, the spectra in the two regimes display similar gross features. At small values of $|a_{BF}|$ the peaks are located near the frequencies of the higher-order monopolar modes, but at larger values they tend to spread over the whole range of frequency. This phenomenon occurs for the same choice of parameters for which the blue shift of the collisional fermionic modes becomes pronounced and several mode crossings occur. For $a_{BF} = -3$ nm the first fermionic peak is strongly blue-shifted while the low-frequency part of the spectrum is dominated by bosonic modes having considerable oscillator strength in both bosonic and fermionic spectral functions. This indicates a strong dynamical coupling of the density fluctuations of the two species in a regime of parameters where the uncoupled frequencies are close to the coupled solutions for the collisional fermionic modes (see again Fig. 1). A careful analysis also shows that for $a_{BF} = -3$ nm the frequencies of the bosonic modes in the RPA spectra are slightly red-shifted, showing the first indications of a trend towards softening on the approach to collapse.

Finally, in Fig. 5 we compare the collisional results for the monopolar spectral function (bottom panel) with those of the RPA (top panel) for a ${}^{87}\text{Rb}-{}^{40}\text{K}$ mixture with the same choice of parameters as in Fig. 2. The RPA spectra show a fragmented fermionic contribution around the frequency $2\omega_F$ of the bare monopolar oscillation as well as two main bosonic peaks at its sides. The frequency of these two peaks tends to decrease with increasing N_B , similarly to what is found for the same modes in the collisional regime. This suggests that such frequency softening is a signature of the incipient collapse.

V. SUMMARY AND CONCLUDING REMARKS

In summary, we have used the equations of generalized hydrodynamics to study the collective modes of trapped boson-fermion mixtures with mutual attractive interactions driving the mixture towards the collapse instability. We have focused on two specific systems of experimental interest, for which we have chosen two different routes to collapse.

In both cases we find that the collective spectra show a frequency softening of a family of modes of bosonic nature as a signature of the incipient collapse. This softening becomes most pronounced in a very narrow region of parameters near collapse. A second effect of increasing the attractive coupling between the two species is a blue shift of the modes of fermionic origin, which becomes more evident for large numbers of bosons and reflects the compression of the fermionic cloud from the interactions with the bosons.

A comparison of the hydrodynamic spectra with the spectra calculated in the collisionless regime within the random-phase approximation suggests that both the blue shift of the “fermionic” modes and the softening of the “bosonic” modes are general features of the dynamics of the mixture. By comparing the height of the peaks in the bosonic and fermionic spectral functions we also conclude that the two families of modes can be most efficiently excited by applying the driving fields separately on the species.

Our analysis has been restricted to the linear regime, neglecting nonlinear and beyond-mean-field effects which may start to play a role close to collapse. We hope to address these issues in future work.

Acknowledgments

This work was partially supported by INFM through the PRA-Photonmatter Program.

APPENDIX: SPECTRAL FUNCTIONS IN THE COLLISIONAL REGIME

The spectral functions of a mixture in the collisional regime can be obtained by adding the perturbing fields $\delta U_\sigma(\mathbf{r})e^{i\omega t}$ to the trapping potential $V_\sigma(\mathbf{r})$ in Eqs. (1) and (2) and then linearizing the equations of motion in terms of the induced density fluctuation $\delta\rho_\sigma(\mathbf{r},\omega)$. This leads in Fourier transform with respect to time to the equation

$$m_\sigma \omega^2 \delta\rho_\sigma = \nabla \cdot (\rho_\sigma^0 \delta\mathbf{F}_\sigma) - g_{BF} \nabla \cdot (\rho_\sigma^0 \nabla \delta\rho_{\bar{\sigma}}) - \nabla \cdot (\rho_\sigma^0 \nabla \delta U_\sigma) \quad (\text{A.1})$$

for each component of the mixture. Here, at variance from Eq. (7) ω is fixed by the frequency of the drive. Equation (A.1) can be solved by expanding $\delta\rho_\sigma(\mathbf{r},\omega)$ in

the basis of the eigenvectors $\delta\rho_\sigma^i(\mathbf{r})$ of Eq. (7) as

$$\delta\rho_\sigma(\mathbf{r}, \omega) = \sum_i C^i(\omega) \delta\rho_\sigma^i(\mathbf{r}). \quad (\text{A.2})$$

In turn, the expansion coefficients C^i are obtained by projecting Eq. (A.1) into the subspace generated by a given fluctuation $\delta\rho_\sigma^i(\mathbf{r})$. This procedure requires defining a scalar product between two eigenmodes of Eq. (7), which we shall denote by the bracket $\langle\delta\rho^i|\delta\rho^j\rangle$. The projection yields

$$C^i(\omega) = \frac{\langle\delta\rho^i|\nabla\cdot(\rho_\sigma^0\nabla\delta U_\sigma)\rangle}{\omega_i^2 - \omega^2} \quad (\text{A.3})$$

where ω_i is the frequency corresponding to the eigenvector $\delta\rho_\sigma^i(\mathbf{r})$.

A generic scalar product can be written as

$$\langle\delta\rho^i|\delta\rho^j\rangle = \sum_{\sigma,\sigma'} \int d^3r \delta\rho_\sigma^i(\mathbf{r}) w_{\sigma\sigma'}(\mathbf{r}) \delta\rho_{\sigma'}^j(\mathbf{r}) \quad (\text{A.4})$$

where $w_{\sigma\sigma'}(\mathbf{r})$ are suitable weights to be determined.

Here we take for the scalar product (A.4) that of a bosonic and of a fermionic cloud in the Thomas-Fermi limit with vanishing mutual interactions. We thus set $w_{FF} = 2A(\rho_F^0)^{-1/3}/3m_F$ and $w_{BB} = g_{BB}/m_B$ and neglect the off-diagonal weight functions. This choice yields

$$C_\sigma^i(\omega) = \frac{Z_\sigma^i}{\omega_i^2 - \omega^2} \quad (\text{A.5})$$

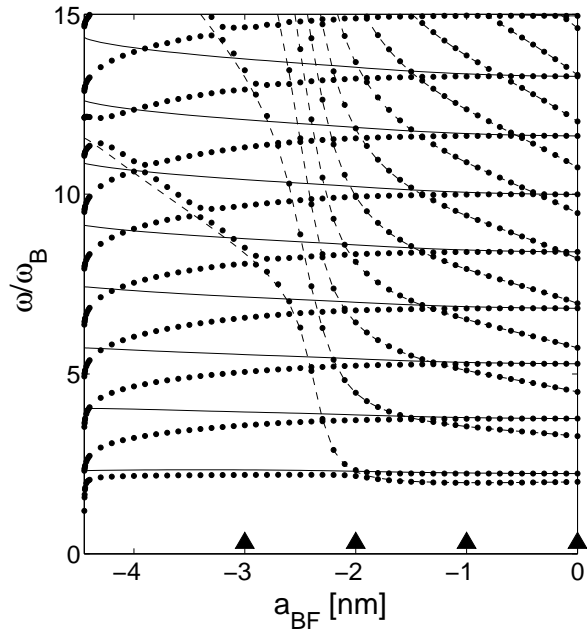
for fermions and bosons, where Z_σ^i is given in Eqs. (9) and (10). We have taken $\delta\rho_\sigma^i$ as normalized to unity ($\langle\delta\rho^i|\delta\rho^i\rangle = 1$).

The spectral functions are then calculated from the definition

$$S_{\sigma\sigma'}(\omega) = -\frac{1}{\pi} \text{Im} \int d^3r \delta U_\sigma^*(\mathbf{r}) \delta\rho_{\sigma'}(\mathbf{r}, \omega) \quad (\text{A.6})$$

where $\delta\rho_{\sigma'}$ is evaluated by setting $\delta U_{\sigma'} = 0$. The use of Eqs. (A.2) and (A.5) in Eq. (A.6) directly leads to Eq. (8) in the main text.

-
- [1] B. DeMarco and D. S. Jin, *Science* **285**, 1703 (1999).
[2] S. R. Granade, M. E. Gehm, K. M. O'Hara, and J. E. Thomas, *Phys. Rev. Lett.* **88**, 120405 (2002).
[3] A. G. Truscott, K. E. Strecker, W. I. McAlexander, G. B. Partridge, and R. G. Hulet, *Science* **291**, 2570 (2001).
[4] F. Schreck, L. Khaykovich, K. L. Corwin, G. Ferrari, T. Bourdel, J. Cubizolles, and C. Salomon, *Phys. Rev. Lett.* **87**, 080403 (2001).
[5] G. Roati, F. Riboli, G. Modugno, and M. Inguscio, *Phys. Rev. Lett.* **89**, 150403 (2002).
[6] Z. Hadzibabic, C. A. Stan, K. Dieckmann, S. Gupta, M. W. Zwierlein, A. Görlitz, and W. Ketterle, *Phys. Rev. Lett.* **88**, 160401 (2002).
[7] K. E. Strecker, G. B. Partridge, and R. G. Hulet, *Phys. Rev. Lett.* **91**, 080406 (2003).
[8] Z. Hadzibabic, S. Gupta, C. A. Stan, C. H. Schunck, M. W. Zwierlein, K. Dieckmann, and W. Ketterle (2003), *cond-mat/0306050*.
[9] H. T. C. Stoof, M. Houbiers, C. A. Sackett, and R. G. Hulet, *Phys. Rev. Lett.* **76**, 10 (1996).
[10] Y. Ohashi and A. Griffin, *Phys. Rev. Lett.* **89**, 130402 (2002).
[11] H. Hu and X.-J. Liu, *Phys. Rev. A* **68**, 023608 (2003).
[12] G. Ferrari, M. Inguscio, W. Jastrzebski, G. Modugno, G. Roati, and A. Simoni, *Phys. Rev. Lett.* **89**, 053202 (2002).
[13] H. Feshbach, *Ann. Phys. (NY)* **19**, 287 (1962).
[14] W. C. Stwalley, *Phys. Rev. Lett.* **37**, 1628 (1976).
[15] E. Tiesinga, B. J. Verhaar, and H. T. C. Stoof, *Phys. Rev. A* **47**, 4114 (1993).
[16] H. Heiselberg, C. J. Pethick, H. Smith, and L. Viverit, *Phys. Rev. Lett.* **85**, 2418 (2000).
[17] M. J. Bijlsma, B. A. Heringa, and H. T. C. Stoof, *Phys. Rev. A* **61**, 053601 (2000).
[18] G. Modugno, G. Roati, F. Riboli, F. Ferlaino, R. J. Brecha, and M. Inguscio, *Science* **297**, 2240 (2002).
[19] T. Miyakawa, T. Suzuki, and H. Yabu, *Phys. Rev. A* **64**, 033611 (2001).
[20] R. Roth and H. Feldmeier, *Phys. Rev. A* **65**, 021603 (2002).
[21] R. Roth, *Phys. Rev. A* **66**, 013614 (2002).
[22] X.-J. Liu, M. Modugno, and H. Hu, *Phys. Rev. A* **68**, 053605 (2003).
[23] M. Modugno, F. Ferlaino, F. Riboli, G. Roati, G. Modugno, and M. Inguscio, *Phys. Rev. A* **68**, 043626 (2003).
[24] P. Capuzzi, A. Minguzzi, and M. P. Tosi, *J. Phys. B: At. Mol. Opt. Phys.* (2003), submitted.
[25] P. Capuzzi, A. Minguzzi, and M. P. Tosi, *Phys. Rev. A* **67**, 053605 (2003).
[26] T. Miyakawa, T. Suzuki, and H. Yabu, *Phys. Rev. A* **62**, 063613 (2000).
[27] X.-J. Liu and H. Hu, *Phys. Rev. A* **67**, 023613 (2003).
[28] R. J. Dodd, M. Edwards, C. J. Williams, C. W. Clark, M. J. Holland, P. A. Ruprecht, and K. Burnett, *Phys. Rev. A* **54**, 661 (1996).
[29] V. M. Pérez-García, H. Michinel, J. I. Cirac, M. Lewenstein, and P. Zoller, *Phys. Rev. Lett.* **77**, 5320 (1996).
[30] T. Sogo, T. Miyakawa, T. Suzuki, and H. Yabu, *Phys. Rev. A* **66**, 013618 (2002).
[31] P. Capuzzi, A. Minguzzi, and M. P. Tosi, *Phys. Rev. A* **68**, 033605 (2003).
[32] K. Mølmer, *Phys. Rev. Lett.* **80**, 1804 (1998).
[33] E. Anderson, Z. Bai, C. Bischof, S. Blackford, J. Demmel, J. Dongarra, J. Du Croz, A. Greenbaum, S. Hammarling, A. McKenney, and P. Sorensen (1999), URL <http://www.netlib.org/lapack>.
[34] W. Kohn, *Phys. Rev.* **123**, 1242 (1961).
[35] J. F. Dobson, *Phys. Rev. Lett.* **73**, 2244 (1994).



[36] P. Capuzzi and E. S. Hernández, Phys. Rev. A **64**, 043607 (2001).

FIG. 1: Monopolar frequencies ω (in units of the bare boson-trap frequency ω_B) of the collisional collective modes as functions of the mutual scattering length a_{BF} (in nm) for a ${}^6\text{Li}$ - ${}^7\text{Li}$ mixture with $N_F = 10^4$ and $N_B = 10^6$. The solid and dashed lines show the frequencies of the dynamically uncoupled modes for bosons and fermions, respectively. The triangles correspond to the values of a_{BF} for which we have performed the RPA calculations of Figs. 3 and 4.

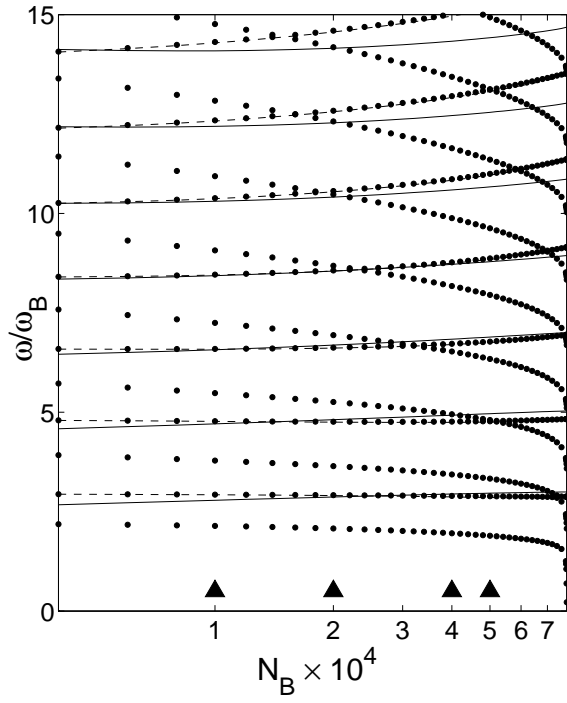


FIG. 2: Monopolar frequencies ω (in units of ω_B) of the collisional collective modes as functions of the number N_B of bosons (in log scale) for the ^{87}Rb - ^{40}K mixture with $N_F = 2 \times 10^4$. The solid and dashed lines show the frequencies of the dynamically uncoupled modes for bosons and fermions, respectively. The triangles correspond to the values of N_B for which we have performed the RPA calculations of Fig. 5.

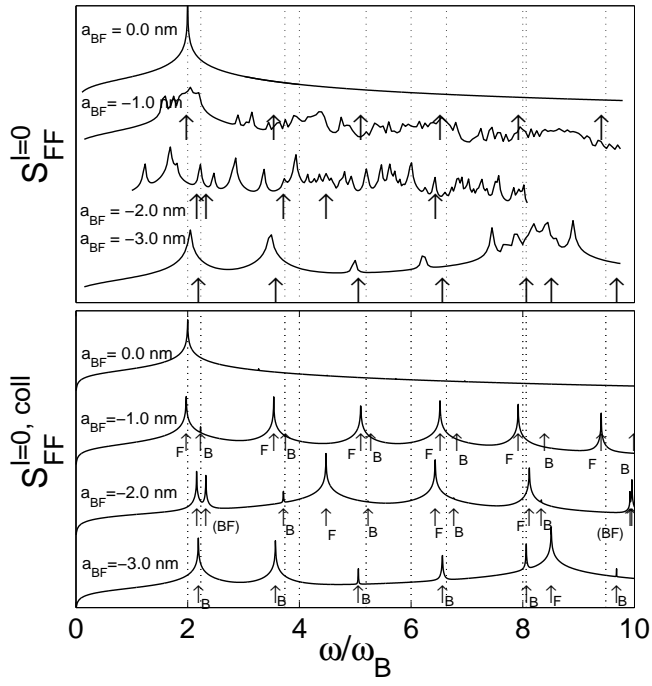


FIG. 3: Monopolar spectrum (in log scale and arbitrary units) for fermions as functions of ω (in units of ω_B) in a ${}^6\text{Li}$ - ${}^7\text{Li}$ mixture with $N_F = 10^4$, $N_B = 10^6$ and for various values of a_{BF} . The spectra are plotted for the sake of clarity with a spectral width of order $10^{-5} \omega_B$. The vertical dotted lines indicate the values of the bosonic and fermionic monopolar modes in the absence of boson-fermion coupling. Top panel: spectral response within the RPA; the arrows indicate the frequencies of the collisional modes with non-negligible spectral weight for the same parameters. Bottom panel: spectral response in the collisional regime; the arrows denote all collisional modes for the same parameters with label B or F to indicate the type of mode as identified from its proximity to an uncoupled collisional mode (the labels BF indicate ambiguous cases).

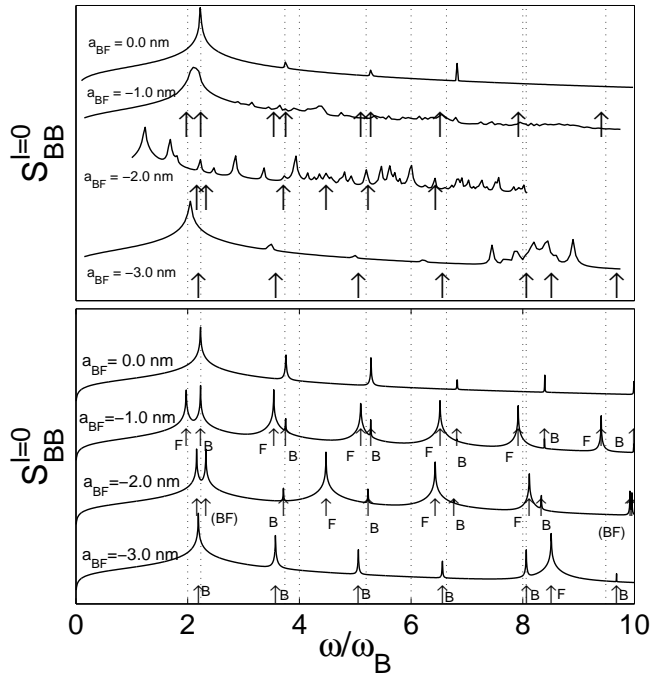


FIG. 4: The same as in Fig. 3 for the bosonic response.

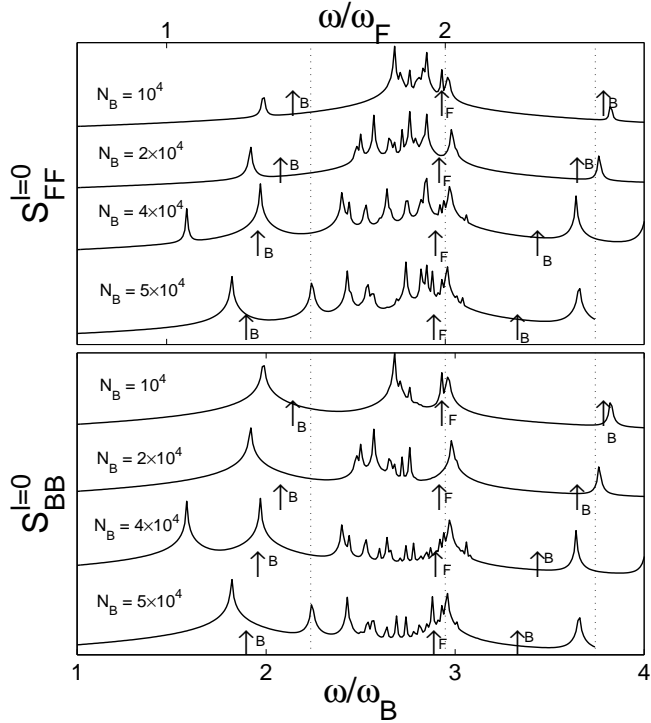


FIG. 5: Monopolar spectral response (in log scale and arbitrary units) from the RPA for fermions (top) and bosons (bottom) as functions of ω (in units of ω_F or ω_B) for a ^{87}Rb - ^{40}K mixture with $a_{BB} = 5.5$ nm, $a_{BF} = -21.7$ nm, $N_F = 2 \times 10^4$, and increasing values of N_B . The arrows indicate the collisional modes for the same parameters. The vertical dotted lines are the values of the bosonic and fermionic monopolar modes in the absence of boson-fermion coupling.